European Journal of Pharmaceutics and Biopharmaceutics 139 (2019) 262–271

Contents lists available at ScienceDirect

European Journal of Pharmaceutics and Biopharmaceutics

journal homepage: www.elsevier.com/locate/ejpb

Research paper

Development and in vitro evaluation of pressure sensitive adhesive patch for the transdermal delivery of galantamine: Effect of penetration enhancers and crystallization inhibition

Dina Ameen[a,b,c], Bozena Michniak-Kohn[a,b,*]

[a] Ernest Mario School of Pharmacy, Rutgers-The State University of New Jersey, 160 Frelinghuysen Road, Piscataway, NJ 08854, USA
[b] Center for Dermal Research, Rutgers-The State University of New Jersey, 145 Bevier Road, Piscataway, NJ 08854, USA
[c] Department of Pharmaceutics, College of Pharmacy, University of Baghdad, Baghdad, Iraq

ARTICLE INFO

Keywords:
Galantamine
Penetration enhancer
Transdermal patch
PSA
Permeation
Alzheimer's disease

ABSTRACT

The transdermal route offers an attractive alternative route of drug administration especially for Alzheimer's disease patients through eliminating gastrointestinal side effects and ultimately improving compliance. In this study, we prepared an optimized matrix–type patches for the transdermal delivery of galantamine free base with ex vivo and in vitro evaluation. Four pressure sensitive adhesives with different functional groups, ten penetration enhancers and four drug loadings were tested to determine the optimized patch. The ex vivo permeation of the different formulated patches through human cadaver skin using vertical Franz diffusion cells showed that GELVA GMS 788 was the best pressure sensitive adhesive among the tested polymers. FT-IR and rheological studies done to investigate any potential interactions of the polymer with the drug and/or additives showed the possibility of hydrogen bonding between the drug and pressure sensitive adhesive (PSA), also the additives had a plasticization effect causing increased flexibility of the polymer chains. The optimized formulation had 10%w/w drug loading, 5% w/w limonene as a penetration enhancer, and 5%w/w oleic acid as a crystallization inhibitor. The combination of limonene and oleic acid increased the flux of galantamine by 2.7-fold compared to 1.7-fold when limonene was used alone. The optimized patch exhibited diffusion release kinetics and fitted well to Higuchi's model and yielded a permeation rate of 32.4 ± 1.41 μg/cm^2/h across human cadaver skin.

1. Introduction

Transdermal drug delivery systems (TDDS) present the active pharmaceutical ingredient(s) (APIs) to the systemic circulation through application of the device on the skin. In this case the APIs are expected to permeate across the skin usually by passive diffusion (some devices utilize non-passive approaches such as iontophoresis or ultrasound) to reach the microcirculation of the skin, and then the systemic circulation [1]. TDDS offer several advantages over other routes of administration, such as avoidance of first pass metabolism and gastrointestinal side effects, non-invasiveness, self-application, controlled drug delivery, etc. [2]. Indeed, passive transdermal patches, a type of TDDS, can reduce the number of doses taken by a patient per day, and some are specifically designed to continuously deliver certain APIs for up to a week [3]. In general, TDD patches are of two types, the reservoir and matrix type of patch. The latter involves dissolving or dispersing the API into an appropriate polymer solution, and then the patch is prepared by solvent evaporation method, and this type of patch is also known as a drug-in-adhesive (DIA) patch [4]. Acrylates, silicones, and polyisobutylene polymers are the most widely used polymers for the preparation of DIA patches. These polymers are also referred to as pressure sensitive adhesives since they provide strong bonding to surfaces upon slight pressure and de-bond without leaving any residue [5]. In addition to forming a matrix to load the API, PSA also provides adhesion to the skin, which is very important to ensure the drug availability for permeation. Furthermore, the choice of PSA plays a critical role in the overall patch performance [6]. Transdermal patches have some superiority among other dosage forms when it comes to convenience of administration especially patients with neurological diseases, such as Alzheimer's disease (AD). AD, a major cause of senile dementia, is characterized by progressive neurodegeneration causing gradual neuronal and memory loss, and cognition impairment [7]. Indeed, adherence to treatment, especially in Alzheimer's disease is crucial for maximal clinical efficacy. However, research reveals that compliance to

* Corresponding author at: 145 Bevier Rd, Piscataway, NJ 08854, USA.
E-mail address: michniak@pharmacy.rutgers.edu (B. Michniak-Kohn).

https://doi.org/10.1016/j.ejpb.2019.04.008
Received 20 July 2018; Received in revised form 6 April 2019; Accepted 11 April 2019
Available online 11 April 2019
0939-6411/

treatment is well below optimum, which can be attributed to several factors. The decline in memory and cognitive function of the patients and reliance on the caregiver to administer the medication are key factors in low adherence [8]. Furthermore, elderly patients usually complain of chronic diseases requiring simultaneous drug therapies along with multiple daily dosing, drug-drug interactions and higher incidence of adverse reaction all predisposing to patient non-compliance [9]. The effects of the aforementioned factors can be alleviated by the use of transdermal patches. Studies have shown that applying transdermal rivastigmine patches resulted in significantly higher caregiver preference and better patient compliance than the oral treatment [10]. These results highlight the need to develop TDDS for other AD drugs in order to maximize their efficacy. Galantamine (GAL) is one of first-line treatments for mild-to-moderate AD with dual mode of action. It is both a selective reversible acetylcholinesterase inhibitor as well as an allosteric nicotinic receptor modulator [11]. GAL was shown to improve patient cognitive and global function, ability to perform activities of daily living and behavior compared to placebo and baseline, and also it reduced caregiver burden [12]. However, it is associated with gastrointestinal side effects and induced weight loss that necessitates gradual increase in dose to improve tolerability [13]. GAL is a tertiary alkaloid with a molecular weight of 287.35 g/mol and log p of 1.8 (PubChem CID: 9651). With such physicochemical properties, and therapeutic profile, it is considered as a good candidate for transdermal delivery.

The objective of this study was to develop a galantamine matrix transdermal patch based on PSA. The final formulation was optimized by selecting the best performing PSA, drug loading, penetration enhancer, and controlling crystallization. The optimized patch formulation was characterized, and the transdermal delivery of the drug was tested using human cadaver skin, which is the golden standard when it comes to testing transdermal flux in vitro. The flux of the drug was used to calculate the predicted steady state plasma levels and confirm attaining therapeutic concentrations in vivo.

2. Materials and methods

2.1. Materials

Galantamine (GAL) was purchased from APExBio (Houston, TX, USA). Limonene (Lim), Terpineol (Terp), and Propandiol (Prop) were purchased from sigma (St. Louis, MO, USA). Borneol (Bor) was purchased from Alfa Aesr (Tewksbury, MA, USA). Labrafac lipophile (Lab), Lauroglycol™ FCC (FCC), caproyl 90 (Cap) are generous gifts from Gattefossé (Paramus, NJ). Oleic acid (OA) was a gift from Croda (Edison, NJ, USA). Oleyl alcohol (OAl), Decyl oleate (DO), and Octyldodecanol (OD) were gifts from BASF (Florham Park, NJ, USA). DURO-TAK 87-900A, DURO-TAK 87-2074, and GELVA GMS 788 were a gift from Henkel Corporation (Bridgewater, NJ). BIO-PSA 7-4202 silicone adhesive was a gift from Dow Corning (Midland, MI, USA). Backing film Scotchpak 9723 and 3 M Scotchpak™1022 release liner were gifts from 3 M Co. (St. Paul, MN, USA). High-performance liquid chromatography (HPLC) grade water, methanol and acetonitrile were purchased from BDH VWR Analytical (Radnor, PA, USA). Dermatomed human cadaver skin was obtained from New York Firefighter Skin Bank (NY, USA).

2.2. Preparation and characterization of drug in adhesive patches

GAL patches were prepared by mechanically mixing the adhesive solution in ethyl acetate with the calculated amount of GAL as a solution in ethyl acetate to prepare 8, 10, 12, and 15% w/w GAL in dry polymer weight. The mixture then was applied onto the release liner using a micrometer adjustable wet film applicator (Zhengzhou TCH Instrument Co., Ltd, China) at a wet film with thickness of 500 μm. Penetration enhancers at 5% w/w of dry polymer weight each were added to the mixture of the polymer and GAL and mixed well and then casted as above. The wet patches were kept at room temperature for 15 min and then baked in a vacuum oven (Model 280A, Thermo Fisher, Waltham, MA, USA) at 80° C for 20 min. The dried patches were laminated with the backing layer and kept at ambient temperature until further testing. The final thickness of the patch was determined using a digital micrometer. Drug content was determined by punching 11 mm disks at different locations of the patch and extracting each by sonication with an appropriate volume of 1:1 mixture of ethyl acetate and methanol for 1 h. Then, the solution was filtered using 0.45 μm syringe filter, diluted appropriately, and analyzed using a validated HPLC method described in the next section. All measurements were performed as triplicates.

2.3. HPLC method of quantification for GAL

Galantamine was quantified using high pressure liquid chromatography (HPLC) with UV detection. The HPLC system included an Agilent 1100 Series Hewlett-Packard liquid chromatograph and the Agilent Chemstation software. The HPLC instrument was equipped with a UV detector (Agilent Dual Absorbance Detector G1315A), a pump (Agilent Quat pump G1311A), and an automatic injector (Agilent ALS G1313A Auto-samplers). A reversed-phase C18 column 5 μm, 4.6 × 150 mm (Xterra, Waters) was used as the stationary phase at a temperature of 25° C. The mobile phase composed of water for HPLC: Methanol (60:40 v/v) with 0.01% triethanolamine with pH adjusted to 5.2 using 85% *o*-phosphoric acid was pumped at a flow rate of 1.2 mL/min. The UV detector was set at a wavelength of 210 nm. The retention time for GAL was 2.5 min. The method was linear at a concentration range 0.5–250 μg/ml with R^2 of 0.999. The limit of detection was found to be 0.22 μg/ml and the limit of quantification (LOQ) was 0.75 μg/ml.

2.4. Ex vivo skin permeation

Frozen dermatomed human cadaver skin was obtained from New York Firefighters Skin Bank (New York, NY). The human cadaver skin pieces were harvested from the posterior torso of three different Caucasian donors (2 males and one female) with age range of 64–69 years. Upon receipt, the skin was kept frozen at −80 °C. On the day of study, the skin was thawed at room temperature, cut into pieces with an appropriate size to fit into the Franz diffusion cells, and hydrated in PBS pH 7.4 for 20 min. The permeation study was conducted using vertical Franz diffusion cells (Logan Instruments, Somerset, NJ). The skin pieces were sandwiched between the donors and receptor compartments with the stratum corneum facing upward toward the donor. Then, the whole assembly was clamped tightly. The receptor compartments were filled with 5.0 mL 5% ethanol in PBS (pH 7.4, 20 mM) maintained at 37 °C using a heating block and stirred continuously at 600 rpm. The diffusion cell area was 0.64 cm^2. Patches of appropriate size were cut using scissors and applied on top of the skin. At predetermined time points (2 h, 4 h, 6 h, 10 h, 11 h, 22 h and 24 h), 0.3 mL of the receptor compartment was withdrawn and replaced immediately with an equal volume of fresh receptor medium. The withdrawn samples were analyzed using HPLC to determine GAL concentrations. All experiments were performed with 3–4 replicates.

2.5. Microscopic examination

Patches used for studying the crystallization of the drug were kept at room temperature in a closed container without lamination with a backing layer. The patches were visualized using Leica S8APO stereomicroscope equipped with an MC170 HD camera (Leica Microsystems, Inc., Chicago, IL, USA) at day 1, and every week for 4 weeks to investigate the potential of crystallization of GAL.

2.6. GAL release study

The release of GAL from selected patches was studied using vertical Franz diffusion cells (Logan Instruments, Somerset, NJ) mounted with a dialysis membrane with MWCO of 2 K Da. Patches 10 mm in diameter were applied onto the dialysis membrane and the receptor medium was 5.0 mL 5% ethanol in PBS (pH 7.4, 20 mM) maintained at 37 °C using a heating block and stirred continuously at 600 rpm. At 0.25, 0.5, 0.75, 1, 1.5, 2, 4, 6, 10, 20, 24 h, 0.3 mL samples were withdrawn and replenished by an equal volume of fresh medium. The samples were analyzed using HPLC to quantify the amount of GAL released. The cumulative amount released per unit of surface area was plotted against time and fitted to several models including, Higuchi equation, first order, and zero order equations to obtain the best fit model [14–15]

2.7. FT-IR studies

The FT-IR spectra of neat GAL, PEs, PSA, and patch formulations containing 10% GAL with or without PE were evaluated with Nicolet iS10 FT-IR Spectrometer (Thermo Fisher, Waltham, MA, USA). The samples were tested by applying a small quantity of GAL powder, or a drop of tested liquid sample (solutions of PSA and patch formulations in ethyl acetate) on top of the lens. The spectra were obtained at a resolution of 4 cm^{-1} from 4000 to 500 cm^{-1}.

2.8. Rheology

Rheological measurements were performed with Kinexus rotational rheometer (Malvern instruments, Malvern, UK) using an 8 mm flat stainless steel plate. All tests were done at 32° C and a gap of 500 μm. The linear viscoelastic region (LVR), where the material usually behaves as an elastic solid, was determined at the strain range of 1–100% with a frequency of 1 Hz. Frequency sweeps were done by oscillating the samples at angular velocity (ω) range of 0.1–100 rad/sec and a stress of 1000 pa within the LVR. Elastic and viscous moduli, G', and G'', as well as tan δ as a function of ω were recorded.

2.9. Data analysis

The individual permeation profile of each formulation was obtained by plotting the cumulative amounts of GAL permeated per unit skin area versus time. The flux (J) represents the slope of the linear portion of the plot, which is determined by the linear segment having the highest linearity coefficient value (R^2). The lag time is equal to the x-axis intercept of the extrapolated linear portion of the permeation profile. The enhancement ratio (ER) was calculated according to Eq. (1):

$$ER = \frac{J \text{ with the enhancer}}{J \text{ without enhancer}} \quad (1)$$

All data are expressed as mean ± standard deviation of three-four replicates. ANOVA and Student's t-test were used to test the level of significance. Results were considered statistically significant at p-value < 0.05.

3. Results and discussion

3.1. The effect of PSA on GAL permeation

Polymers selection plays a crucial role in designing matrix type transdermal patches. These polymers are integral not only to the performance, but also to the physicochemical stability of the transdermal patches [4,6]. Four different polymers were tested in this study to determine their compatibility with GAL, drug loading capacity and effects on the skin permeation of GAL. Table 1 lists the tested polymers along with their chemical composition and functional groups. The acrylate polymers tested had either no functional group, a hydroxyl group, or a combination of −COOH and −OH. On the other hand, the tested silicone polymer was specifically designed to be compatible with amine containing molecules. Initially, the suitability of the polymer was tested by studying the permeation of GAL from patches at a drug loading of 8% w/w of dry polymer. The results of the permeation study shown in Fig. 1 demonstrate that the drug had higher permeation rate with the PSA containing −OH than other adhesives used. In addition, the acrylate PSAs were better than the silicone polymer for delivering GAL. Although the tested silicone adhesive was specifically designed to be compatible with amine compounds, it showed discoloration after oven drying, which was considered as a sign of incompatibility with GAL. PSAs with −COOH functional group are known to interact with amine containing compounds through hydrogen bonding between the −COOH and the amino group of APIs reducing their skin permeation [16–17]. GELVA GMS 788 exhibited the highest permeation of GAL among the tested polymers. Therefore, GELVA GMS 788 was selected as the polymer of choice for further experimentation.

3.2. The effect of GAL loading on permeation

The effect of GAL loading on the skin permeability of the API was studied by preparing different GAL concentrations in GELVA GMS 788 (8, 10, 12, and 15% w/w of dry polymer weight). Fig. 2 depicts the permeation profile of GAL from patches with different loadings. Data (see Table 2) showed that 10% w/w had the highest cumulative amount permeated through human cadaver skin. It is anticipated that the flux would increase directly with the increase in sub-saturation drug loading. However, upon close examination, the patches with 15 and 12% w/w GAL loadings were found to have extensive crystallization (data not shown). Saturation of the drug in a vehicle is important to maximize the thermodynamic activity. On the contrary, crystallization of the drug within the PSA matrix reduces the thermodynamic activity causing a reduction in skin permeation [18–19]. Furuishi et al. demonstrated that the transdermal permeation of pentazocine from acrylate adhesive patches increased with drug loading to a maximum of 30% followed by a reduction at higher drug concentration. The results were attributed to the crystallization of pentazocine at higher loading levels [20]. Our results are consistent with the previously published literature in that crystallization may be responsible for the observed reduction in GAL permeation. As a result, the saturation solubility of GAL in GELVA GMS 788 was considered to be around 10% w/w, and hence this drug loading was used for further optimization.

3.3. The effect of penetration enhancers on GAL permeation

Several strategies have been developed to tackle the powerful barrier function imposed by the stratum corneum (SC). One of the methods is to include chemical penetration enhancers (PEs) in the formulation. These enhancers increase the permeability of drugs by different mechanisms including disruption of the lipid bilayer, fluidization, extraction of stratum corneum lipids, etc. [21]. The inclusion of PEs into patches not only affects the permeation of the drug, but it might also influence its release [22]. In order to further increase the permeability of GAL through the skin, ten PEs were tested at 5% w/w of dry polymer weight, fixing GAL at 10% w/w loading. The PEs tested belonged to different categories regarding their chemical properties and anticipated mechanism of action. Fig. 3 depicts the permeation rates of GAL from matrices containing different PEs, and Table 3 shows the relevant permeation parameters. Among the tested PEs, Labrafac lipophile (Lab), lauroglycol™ FCC (FCC), and caproyl 90 (Cap) did not show a significant enhancement of GAL flux, while propandiol (Prop) slightly reduced the permeation of GAL. On the other hand, limonene (Lim), terpineol (Terp), borneol (Bor), oleyl alcohol (OAl), octyldodecanol (OD), and decyl oleate (DO) showed a higher flux than that of the control (GAL patch without enhancer). Lim, Terp, and Bor belong to the

Table 1
List of tested PSAs with their chemical composition and in vitro skin permeation parameters of 8% GAL loading across human cadaver skin using (n = 3).

Adhesive	Chemical composition	Functional group	Flux (μg/cm^2/h) ± SD	R^2 [a]	Q_{24} (μg/cm^2) ± SD
DURO-TAK 87-900A	acrylates copolymer	None	2.25 ± 0.5	0.9893	55.56 ± 1.7
DURO-TAK 87-2074	acrylates copolymer	−COOH/−OH	1.00 ± 0.8	0.9969	32.62 ± 17
GELVA GMS 788	acrylates copolymer	−OH	6.00 ± 0.9	0.9967	151.1 ± 24
BIO-PSA 7-4202	Silicon adhesive	–	1.15 ± 0.4	0.9823	26.92 ± 7.0

[a] R^2, linearity coefficient of the flux.

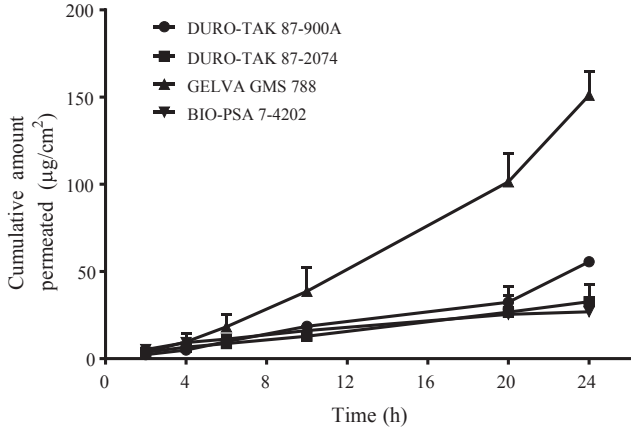

Fig. 1. The effect of pressure sensitive adhesive type on the permeation of galantamine across human cadaver skin at 8% w/w drug concentration (mean ± S.D., n = 3).

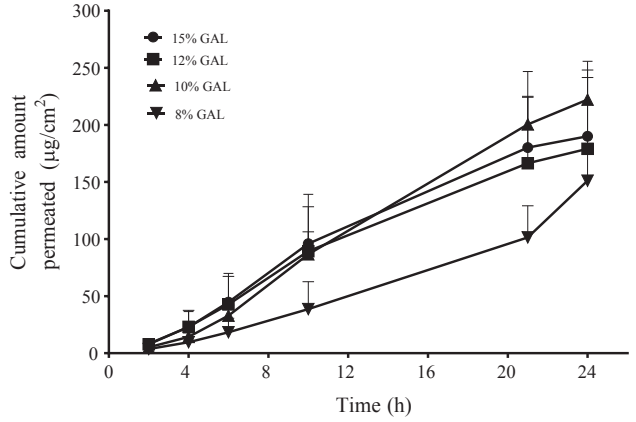

Fig. 2. The effect of drug loading in GELVA GMS 788 on the permeation of galantamine across human cadaver skin (mean ± S.D., n = 3).

Table 2
In vitro skin permeation parameters of GAL from GELVA GMS 788 patches containing different drug loading amounts through human cadaver skin using (n = 3–4).

Drug Loading %(w/w)	Flux (μg/cm^2/h) ± SD	Q_{24} (μg/cm^2) ± SD	R^2 [a]	Lag time (h) ± SD
8	6.00 ± 0.9	151.0 ± 19.4	0.9967	2.8 ± 1.1
10	12.2 ± 2.8	235.0 ± 4.0	0.9976	3.0 ± 0.1
12	11.1 ± 0.5	201.9 ± 52	0.9847	2.0 ± 1.0
15	13.9 ± 0.4	214.8 ± 53	0.986	2.4 ± 0.8

[a] R^2, linearity coefficient of the flux.

family of terpenes, which are naturally occurring volatile oils widely used and tested as PEs [23]. Generally, terpenes competitively make hydrogen bonds with skin ceramides causing disruption of the lipid

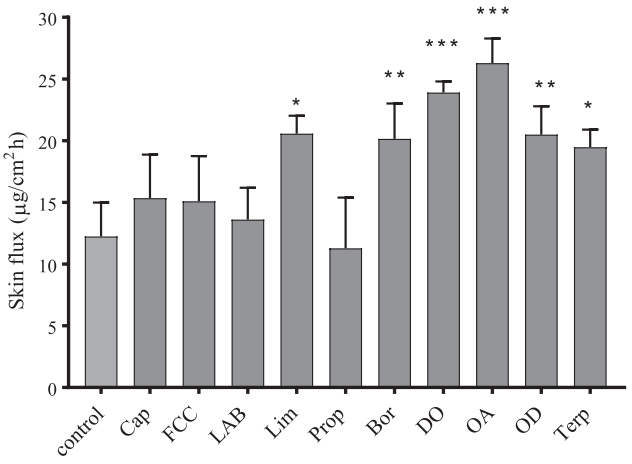

Fig. 3. The flux of galantamine from GELVA GMS 788 patches containing different PEs through human cadaver skin (mean ± S.D., n = 3–4).

packing in the SC resulting in increased permeability of active molecules [24]. The results showed that all tested terpenes significantly enhanced the permeation of GAL as compared to control patch without PE. Also, it was shown that Lim had significantly reduced the lag time more than did the other two terpenes. The reduction in the lag time indicates an increased diffusivity of the drug. This behavior of Lim was attributed to its lipophilicity, which favors its fast permeation through the skin [25–26]. OAl and OD are unsaturated fatty acid and aliphatic fatty alcohol, respectively. These long chain lipophilic molecules act as PE by fluidizing the SC lipids through interactions with the lipid layer boundary phospholipids and reducing the barrier integrity [27–28]. The present study shows that OAl resulted in the highest GAL flux amongst all other PEs tested. Agyralides et al. showed that the incorporation of 10% w/w OAl increased the permeation of furosemide from gels by 25-fold. OAl enhancement property was attributed to the presence of a double bond causing a kink in its molecular structure that can disrupt the SC lipid packing [29]. Whereas, OD was shown to increase the flux of formoterol fumarate from ethylene vinyl acetate matrix patches by 6.3-fold across human skin. When incorporated into acrylate PSA patches, fatty alcohols act as plasticizers for the polymer. They enhance the polymer flexibility and drug molecules mobility facilitating the latter release from the polymer matrix. Hence, more drug molecules would be available for permeation [30]. The best enhancers of the two PE groups were chosen for further investigations, namely Lim, and OAl.

3.4. Drug crystallization

Crystallization of the API represents a critical issue for the stability of matrix patches. It also adversely impacts the delivery of the drug [31].The prepared patches were examined under the microscope one day after preparation and every week until the end of 1 month or until signs of crystallization appeared, whichever came first. Patches containing FCC, Lim, Lab, and Prop did not show any signs of crystallization after 4 weeks of storage at room temperature. On the other hand, formulations containing DO, OD, Bor, Trep, and OAl showed

Table 3
Ex vivo skin permeation parameters of GAL from GELVA GMS 788 patches containing different PEs at 5% w/w through human cadaver skin using (n = 4).

Formulation	Flux (μg/cm^2/h) ± SD	Q_{24} (μg/cm^2) ± SD	R^2 [a]	Lag time (h) ± SD	ER [b]
Control	12.2 ± 2.8	235.0 ± 4.2	0.9967	3.0 ± 0.1	–
Limonene *(Lim)*	20.6 ± 1.3	255.5 ± 55	0.9986	2.2 ± 0.3	1.7
Terpineol *(Terp)*	19.5 ± 0.5	281.0 ± 19	0.9603	3.4 ± 0.2	1.6
Borneol *(Bor)*	20.1 ± 1.2	288.0 ± 40	0.9909	2.5 ± 0.3	1.7
Oleyl alcohol *(OA)*	26.3 ± 1.4	349.0 ± 25	0.999	2.1 ± 0.1	2.2
Labrafac lipophile *(Lab)*	13.6 ± 1.0	202.2 ± 30	0.9949	3.4 ± 0.2	1.1
Caproyl 90 *(Cap)*	15.4 ± 1.5	193.6 ± 33	0.9975	3.0 ± 0.5	1.3
Propandiol *(Prop)*	11.3 ± 2.0	157.5 ± 43	0.9994	2.1 ± 0.3	0.9
Lauroglycol FCC™ *(FCC)*	15.1 ± 1.7	190.0 ± 42	1.00	2.5 ± 0.3	1.2
Docyl oleate *(DO)*	24.0 ± 1.0	333.5 ± 7.4	0.9944	2.5 ± 0.2	2.0
Octyl dodecanol *(OD)*	20.5 ± 1.6	297.2 ± 27	0.9971	2.5 ± 0.5	1.7
Olyel alcohol + Oleic acid *(OAl + OA)*	25.0 ± 0.7	344.4 ± 75	0.9991	1.8 ± 0.5	2.0
Limonene + Oleic acid *(Optimized Patch)*	32.4 ± 1.4	466.7 ± 56	0.9954	2.4 ± 0.2	2.7

[a] R^2, linearity coefficient of the flux.
[b] ER, enhancement ratio.

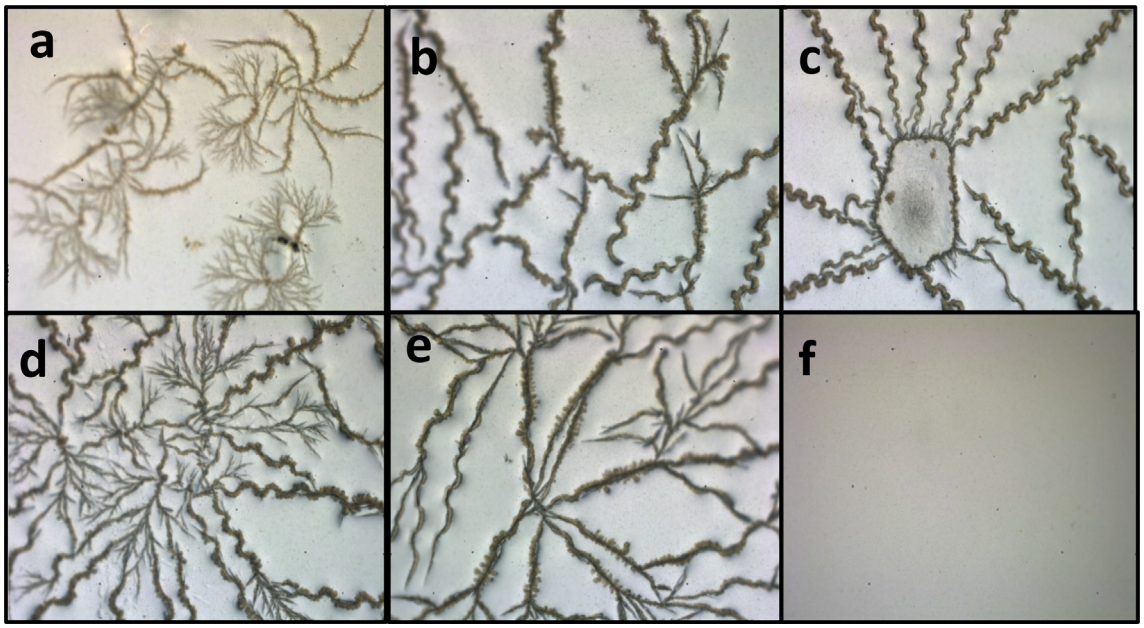

Fig. 4. Galantamine crystallization study in Gelva PSA at 10% w/w drug loading after one week with (a) oleyl alcohol (OAl), (b) borneol (Bor), (c) decyl oleate (DO), (d) Octyldodecanol (OD), (e) terpineol (Terp), and (f) no additives.

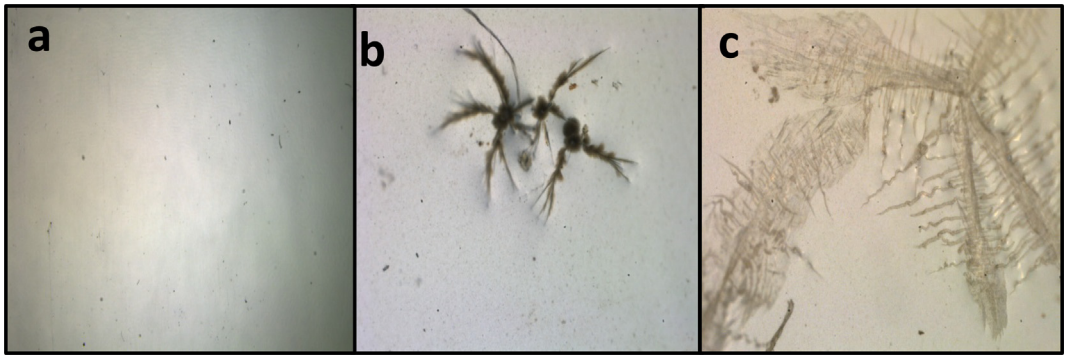

Fig. 5. Galantamine crystallization study in Gelva PSA at 10% w/w drug loading with 5% w/w oleic acid as crystallization inhibitor after 3 weeks with (a)limonene, (b) oleyl alcohol, (c) no additives.

signs of crystallization in less than a week after preparation as shown in Fig. 4. The PE free GAL patch showed crystallization after 3 weeks (Fig. 5 (c)), suggesting that 10%w/w GAL was above saturation level. Weng et al. reported the increased crystallization of risperidone in acrylate PSA matrices upon the addition of various compounds as crystallization inhibitors. They suggested that compounds with OH group tend to reduce the lipophilicity of the PSA, which might reduce the solubility of the drug in the PSA matrix resulting in crystallization of the drug [19]. Further, OAl was shown to enhance the crystallization of Ibuprofen when included in the formulation of multiple polymer

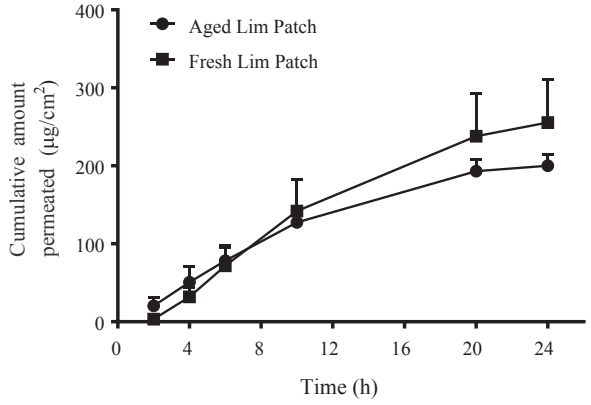

Fig.6. The effect of aging (6 weeks) on the permeation profile of GAL galantamine from GELVA GMS 788 patches containing 5%w/w Limonene as a penetration enhancer. (mean ± S.D., n = 3–4).

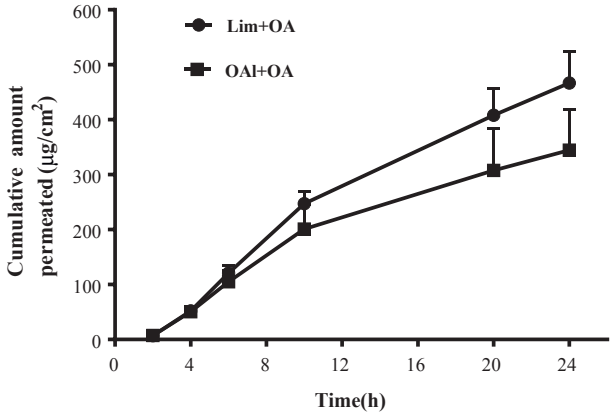

Fig.7. The effect of 5% w/w oleic acid on the permeation rate of galantamine from GELVA GMS 788 patches containing 5% w/w of either Limonene or oleyl alcohol as penetration enhancers across human cadaver skin. (mean ± S.D., n = 4).

adhesive system as a surfactant [32]. Crystallization is likely to initiate in supersaturated systems with the formation of a nucleation of drug molecules that is too big and thus hard to re-dissolve [33]. However, it may take some time for the crystals to grow due to the high viscosity of the PSA matrices. As mentioned earlier, crystallization is a critical issue in transdermal patches formulation, as it directly affects the amount of drug delivered through the skin, besides its negative impact on the esthetics of the product that will impact the patient's acceptability. Since patches with Lim produced high flux and were crystal free for 4 weeks, these presented a good candidate for further investigation. The permeation of GAL from the same batch of the Lim patches was tested again at 6 weeks to examine the effect of aging on the permeation profile of the drug and the results are shown in Fig. 6. Surprisingly, the permeation of GAL was reduced, although no signs of crystallization were found at 4 weeks. Moreover, the flux of GAL was significantly lower after 6 weeks than when fresh (12.72 ± 0.93, and 20.6 ± 1.28 µg/cm2/h, respectively). These results suggested that crystallization of the drug happened at a slower rate, and there is a need to include a crystallization inhibitor. Excipients that inhibit the crystallization of drugs in PSA matrices are proposed to do so by several mechanisms: (i) increasing the solubility of the drug in the matrix, (ii) adsorption onto the drug crystals halting further nuclei growth, or (iii) formation of solid solution with the drug, i.e., amorphous co-precipitates [34]. Oleic acid (OA) was tested for its ability to inhibit the crystallization of GAL. The patches with highest flux values were chosen for this purpose and OA was added at 5%w/w of dry polymer weight into formulations containing either Lim or OAl. Fig. 7 shows the permeation profile of GAL from the freshly prepared patches containing OA as crystallization inhibitor. Interestingly, the addition of OA resulted in dramatic increase in the flux of GAL from Lim + OA patches. On the other hand, there was a small reduction in the flux with OAl + OA patches, although not statistically significant as shown in Table 3. Further, the microscopical examination revealed that OAl + OA patches showed crystallization after 3 weeks (Fig. 5(b)), unlike Lim + OA, which did not show any signs of crystallization for more than 3 months. OA, a fatty acid, is an extensively studied PE, which could also function as a crystallization inhibitor in the PSA matrix patches [19]. Interestingly, OA acted synergistically with Lim to enhance the permeation of GAL besides being effective crystallization inhibitor. However, this OA behavior was not observed when combined with OAl. Such enhancement synergy was also observed with a combination of OA and terpenes for the transdermal delivery of zidovudine, and may be attributed to a combined effect of each enhancer's mechanism of interaction with the SC and/or enhanced solubilization of drug [35–36]. The crystallization inhibitory effect of OA may be attributed to interaction between its carboxyl group and the amine group of GAL that improved the solubility of the drug into the PSA matrix. However, it seems that the presence of Lim has a crucial role for the effective crystallization inhibition of OA. Therefore, a composition of 10% w/w GAL, 5% w/w of each of Lim and OA in GELVA GMS 788 represented a good candidate for further characterization.

3.5. Optimized patch characterization

The ex vivo permeation parameters of the optimized formulation are listed in Table 3. The average patch thickness was found to be 154 ± 2 µm (n = 3). The drug content uniformity of the patch was 99.2 ± 2.3% (n = 3). Further, the permeation of GAL from the optimized patch was repeated after 1 month to determine the effect of aging on drug permeation rate. The results showed that there was no significant difference in the flux of GAL from the same patches after a month of storage at room temperature (30.34 ± 1.99 µg/cm^2 h, n = 4). The plasma steady state concentration (C_{ss}) of GAL can be predicted from its transdermal flux (J) and pharmacokinetic data with the following equation:

$$C_{ss} = \frac{A \times J}{Cl}$$

where, A is the surface area of application, Cl is the clearance of the drug. Moreover, we can use the above equation to determine the surface area of the patch required to achieve therapeutic concentration. Based on pharmacokinetic parameters of GAL in healthy volunteers, where Cl and C_{ss} were found to be 20.16 l/h and 34.6 µg/l, respectively [37]. We can predict that a patch of about 20 cm^2 would be sufficient to achieve and maintain the drug concentration within the therapeutic window.

3.6. Drug release

The release of GAL from the candidate formulation was tested and the release profile was depicted in Fig. 8, along with that of control patch. The dramatic increase in the release rate of GAL from the optimized patch can be attributed to changes in the mechanical properties of the matrix due to the inclusion of Lim and/or OA. A similar effect was seen with the release of blonanserin from acrylate PSA patches in the presence of PE as compared to patches without PE [38]. The release data of the optimized patch were fitted to different kinetic models and linear regression coefficient R^2 values were used to determine the goodness of fit of the respective models. The release parameters listed in Table. 4, showed that Fickian diffusion model (Higuchi) was best to describe the kinetics of GAL release from PSA matrix patches regardless of the inclusion of PE (Fig. 9). Additionally, a mild burst effect was

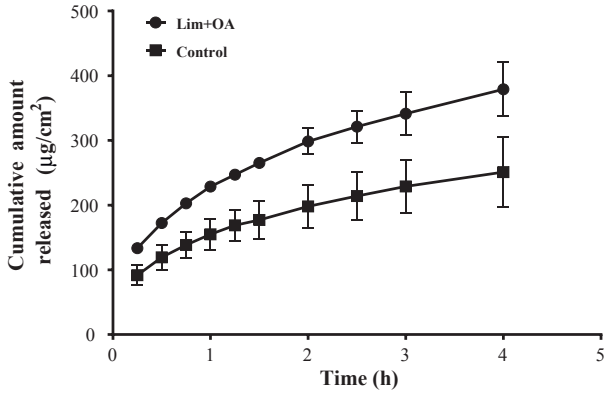

Fig.8. The release profile of galantamine of from GELVA GMS 788 patches with 5% w/w of limonene and oleic acid and control patch (without PE). (mean ± S.D., n = 3).

Table 4
Different release models of galantamine from optimized patch (n = 3).

Model	Equation[a]	K	R²[b]
Zero order	$Q_t = Q_0 + Kt$	62.85 µg/cm²/h*	0.939
First order	$logQ_t = logQ_0 + \frac{Kt}{2.303}$	0.25/h*	0.8491
Higuchi	$Q_t = K_H\sqrt{t}$	164.0 µg/cm²/h½*	0.995

[a] Q_t, amount released at time t; Q_0, amount at time 0; K, release rate constant; t, time.
[b] R^2, linearity coefficient.
* Extremely statistically significant difference ($P < 0.05$) from the control patch.

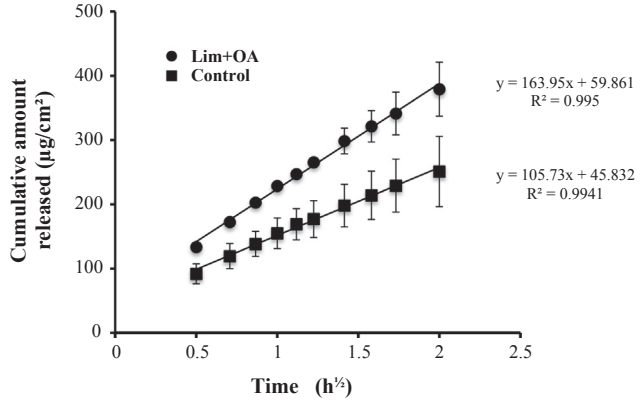

Fig.9. The release amount of galantamine of from GELVA GMS 788 patches with 5% w/w of limonene and oleic acid and control patch (without PE) plotted against the square root of time. (mean ± S.D., n = 3).

noticed in GAL release profile, an effect that could be caused by higher concentration of the drug at the surface of the patch due to its migration along with the solvent during drying phase [39].

3.7. FT-IR study

FT-IR study was conducted to shed light on possible interactions between the PSA, drug, PE and crystallization inhibitor, if any. Fig. 10 shows the spectra of pure GAL with the characteristic broad enolic −OH stretching vibrational peak at 3267 cm^{-1}, $-CH_2$ stretching vibrations at 2800–3000 cm^{-1}. Prominent neat GELVA GMS 788 peaks including C═O stretching vibrations are seen at 1737 cm^{-1} and C−H stretching peaks at 2860–2960 cm^{-1}. Limonene has an out of plane = CH_2 stretching peak at 885.67 cm^{-1}, C═C stretching at 1645 cm^{-1}. Whereas OA has it typical peaks at 1707.88 and 1463.35 cm^{-1} C═O stretching, and out of plane O−H stretching, respectively. Upon mixing GAL with Gelva, the peaks of the former mostly disappeared and only the Gelva spectrum was predominantly detectable. The same observation was noticed with the optimized patch FT-IR spectrum. Fig. 11-(A) compares the FT-IR spectra of GAL, Gelva, and the formulation of their mixture, where it can be clearly seen that all peaks in the region 2800–3400 cm^{-1} of GAL have disappeared including the enolic −OH stretching vibration, which could be attributed to the peaks of the lower fraction component (GAL) being masked by the larger fraction component (PSA). Therefore, at the current setting it might be hard to confirm that any interactions were taking place with the PSA. On the other hand, Gelva maintained its −C−H stretching vibration peaks pattern. However, the peak at 2931.98 cm^{-1} showed a slight shift in the presence of GAL to 2936 cm^{-1}, which could be due to interactions between the drug and the PSA. Mufamadi et al. also reported the disappearance of GAL O-H stretching peak upon encapsulation into liposome, attributing it to interaction between the drug and the liposomes [40]. In addition, Fig. 11 (B) shows the spectra for formulations containing GAL with and without Lim + OA, which did not show any difference from the GAL control except for a slight shift of C-H stretching peak from 2936 to 2934 cm^{-1}, which is closer to the original peak of Gelva seen at 2931.98 cm^{-1}. This might indicate some interactions taking place between Lim and/or OA and GAL that disrupted the interactions between the latter and Gelva. Such hypothetical interaction could be further supported by the crystallization inhibition, release improvement and enhanced permeation. These results were similar to the data reported by Weng et al., who demonstrated that excipients reduced the interactions between risperidone and PSA as manifested by returning FT-IR peaks back to their original wave numbers after the addition of some fatty acids to the drug in PSA formulation [19].

3.8. Rheology

PSAs are viscoelastic materials, which means that they behave as either liquid or solid depending on the applied shear frequency at certain temperature. This property determines the PSA's skin adhesion [41]. Rheological analysis of the mechanical properties of PSA was used to determine the viscoelastic parameters such as elastic modulus (G') and viscous modulus (G''). (G') corresponds to the solid-like behavior, while (G'') corresponds to the liquid-like behavior of the PSA [42]. Ideally upon the application of the patch, the PSA should exhibit a liquid-like behavior so that it has enough flowability allowing close contact with the skin to bond. On the other hand, debonding requires the PSA to behave more like a solid and to demonstrate more cohesiveness. In other words, tack required for boding occurs at lower frequencies, and is associated with a larger (G''). On the contrary, the process of debonding (peel) occurs at higher frequencies and is associated with larger a (G'). Further, the study of the mechanical properties of the transdermal patches can highlight some of the interactions between the PSA polymer chain and the drug and/or additives [43]. Indeed, the viscoelastic moduli would increase with increasing polymer chain stiffness and mechanical strength, whereas increased chain flexibility brought about by plasticization is associated with decreasing moduli values [38,44]. Phase angle (δ) is another parameter that is used to study rheological properties of PSA. δ describes the ratio of the lost to stored energy, hence it is expected to be high at both lower and higher frequencies. The larger the angle the more flexible the polymer [38]. Oscillation frequency sweep results are depicted in Fig. 12 and are consistent with acceptable behavior of PSA. Fig. 12-(A) shows a small reduction in G′ for the optimized patch relative to blank PSA. This reduction, although very small, might indicate some plasticization effect due to Lim and OA reducing chain stiffness and cohesion. The latter observation is backed by the increase in δ for the optimized patch compared to blank PSA and GAL containing patch (Fig. 12-(C)). Similar

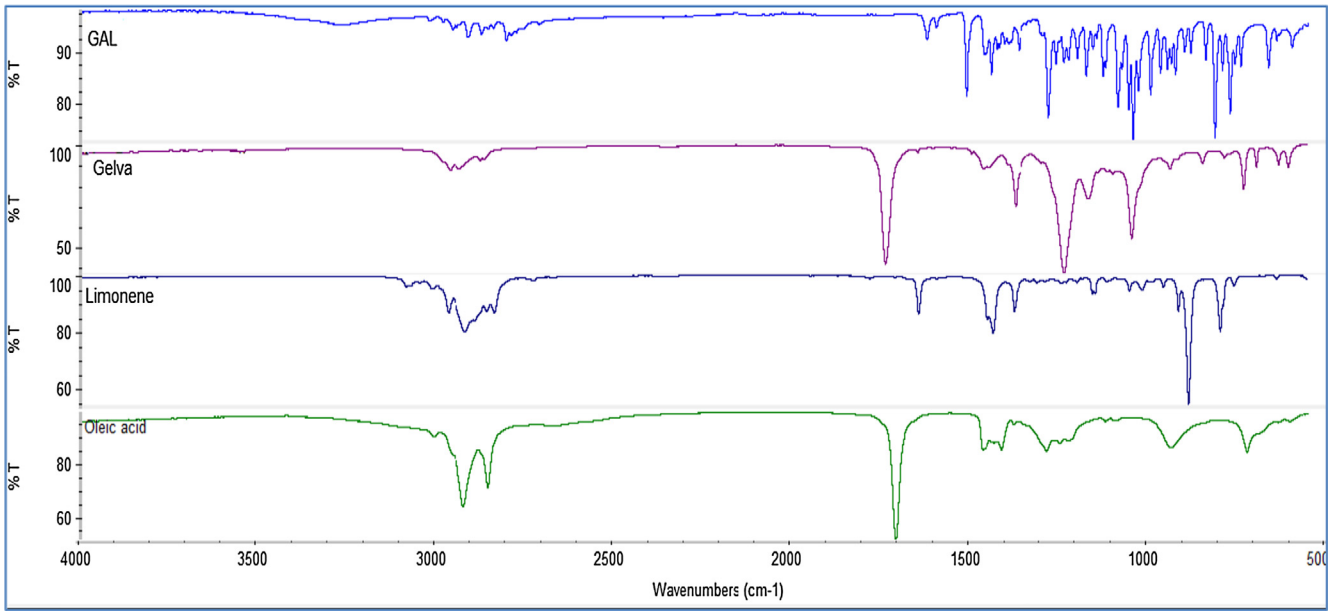

Fig. 10. FT-IR spectra of neat galantamine, Gelva, limonene, and oleic acid.

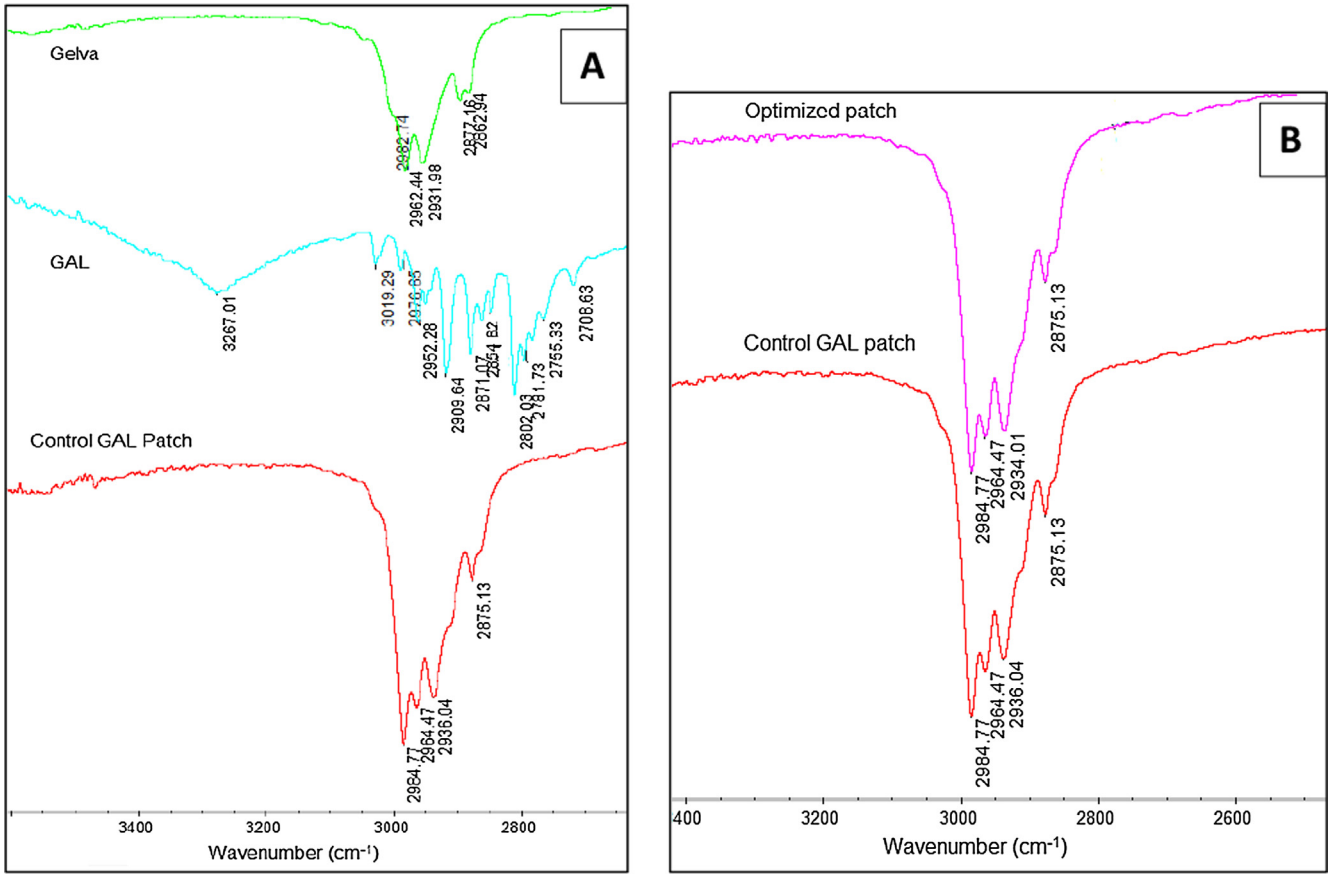

Fig. 11. Comparison of FT-IR spectra of (A) neat galantamine, Gelva, with control galantamine patch formulation , (B) Control galantamine and optimized patch formulations.

rheological behavior was observed with other acrylate PSAs upon incorporation of olanzapine and the penetration enhancer [43].

4. Conclusion

The results of the present study emphasize the importance of selecting a suitable combination of PSA, drug loading, PE, and crystallization inhibitor for the development of transdermal patches with optimum performance. The optimized patch was composed of 10% w/w GAL, 5%w/w Lim, 5% w/w OA, GELVA GMS 788 as PSA, and was casted on Scotchpak^{TM}1022 release liner and laminated with Scotchpak 9723 as a backing film. The selected additives showed a synergistic

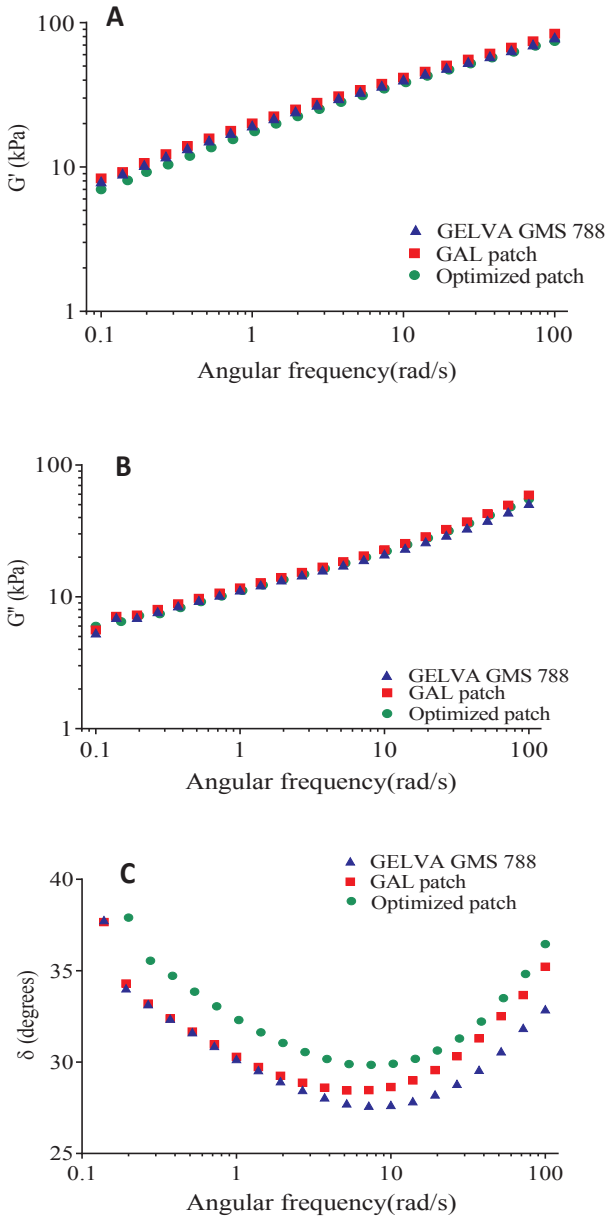

Fig. 12. Oscillation frequency sweep data of blank PSA, 10% w/w galantamine containing PSA, and optimized patch. The elastic modulus (A), the viscous modulus (B), and phase angle (C) were plotted against angular frequency.

enhancement of GAL permeation while successfully inhibiting the drug crystallization. Based on the ex vivo permeation studies using human cadaver skin, the optimized patch produced a steady state flux of Gal that is capable of achieving therapeutic plasma level patch size of about 20 cm^2, which indicates that GAL transdermal patch was a promising drug delivery system for the treatment of Alzheimer's disease. Further pharmacokinetic and in vivo studies should be conducted to confirm the results.

Acknowledgements

Funding for this study was provided by the Center for Dermal Research CDR at Rutgers, The State University of New Jersey, USA. The authors gratefully acknowledge the generous donations provided by BASF, Henkel Inc., Dow Corning, 3 M and the Gattefossé Corporation.

References

[1] A.C. Watkinson, M.-C. Kearney, H.L. Quinn, A.J. Courtenay, R.F. Donnelly, Future of the transdermal drug delivery market – have we barely touched the surface? Expert Opin. Drug Deliv. 13 (4) (2016) 523–532.
[2] Z.A. Alkilani, C.M.T. McCrudden, F.R. Donnelly, Transdermal drug delivery: innovative pharmaceutical developments based on disruption of the barrier properties of the stratum corneum, Pharmaceutics 7 (4) (2015).
[3] S. Wiedersberg, R.H. Guy, Transdermal drug delivery: 30+ years of war and still fighting!, J. Control. Release 190 (2014) 150–156.
[4] S. Kandavilli, V. Nair, R. Panchagnula, Polymers in transdermal drug delivery systems, Pharm. Technol. 26 (5) (2002) 62–81.
[5] F. Cilurzo, C.G.M. Gennari, P. Minghetti, Adhesive properties: a critical issue in transdermal patch development, Expert Opin. Drug Deliv. 9 (1) (2012) 33–45.
[6] S. Lobo, S. Sachdeva, T. Goswami, Role of pressure-sensitive adhesives in transdermal drug delivery systems, Ther Deliv. 7 (1) (2016) 33–48.
[7] S.-Y. Hung, W.-M. Fu, Drug candidates in clinical trials for Alzheimer's disease, J. Biomed. Sci. 24 (2017) 47.
[8] M. Riepe, J. Weinman, J. Osae-Larbi, A. Mulick Cassidy, S. Knox, R. Chaves, et al., Factors associated with greater adherence to and satisfaction with transdermal rivastigmine in patients with Alzheimer's disease and their caregivers, Dement. Geriatr. Cogn. Disord. 40 (1–2) (2015) 107–119.
[9] A.L. Chan, Y.W. Chien, Lin S. Jin, Transdermal delivery of treatment for Alzheimer's disease: development, clinical performance and future prospects, Drugs Aging. 25 (9) (2008) 761–775.
[10] M.C. Pai, H. Aref, N. Bassil, N. Kandiah, J.H. Lee, A.V. Srinivasan, et al., Real-world evaluation of compliance and preference in Alzheimer's disease treatment, Clin Interv Aging. 10 (2015) 1779–1787.
[11] L.J. Scott, K.L. Goa, Galantamine, Drugs 60 (5) (2000) 1095–1122.
[12] S. Lilienfeld, Galantamine—a novel cholinergic drug with a unique dual mode of action for the treatment of patients with Alzheimer's disease, CNS Drug Rev. 8 (2) (2002) 159–176.
[13] J. Corey-Bloom, Galantamine: a review of its use in Alzheimer's disease and vascular dementia, Int J Clin Pract. 57 (3) (2003) 219–223.
[14] W.I. Higuchi, Analysis of data on the medicament release from ointments, J. Pharm. Sci. 51 (8) (1962) 802–804.
[15] L.I. Soler, A. Boix, J. Lauroba, H. Colom, J. Domenech, Transdermal delivery of alprazolam from a monolithic patch: formulation based on in vitro characterization, Drug Dev. Ind. Pharm. 38 (10) (2012) 1171–1178.
[16] E. Jung, E.Y. Lee, H.K. Choi, S.J. Ban, S.H. Choi, J.S. Kim, et al., Development of drug-in-adhesive patch formulations for transdermal delivery of fluoxetine: In vitro and in vivo evaluations, Int J Pharm. 487 (1–2) (2015) 49–55.
[17] C. Zhang, H. Luo, G. Lin, Z. Zhu, F. Zhang, J. Zhang, et al., Transdermal patches for D-threo-methylphenidate (free base): Formulation aspects and in vivo pharmacokinetics, J. Drug Delivery Sci. Technol. 35 (2016) 50–57.
[18] C. Liu, M. Hui, P. Quan, L. Fang, Drug in adhesive patch of palonosetron: Effect of pressure sensitive adhesive on drug skin permeation and in vitro-in vivo correlation, Int J Pharm. 511 (2) (2016) 1088–1097.
[19] W. Weng, P. Quan, C. Liu, H. Zhao, L. Fang, Design of a drug-in-adhesive transdermal patch for risperidone: effect of drug-additive interactions on the crystallization inhibition and in vitro/in vivo correlation study, J Pharm Sci. 105 (10) (2016) 3153–3161.
[20] T. Furuishi, T. Io, T. Fukami, T. Suzuki, K. Tomono, Formulation and in vitro evaluation of pentazocine transdermal delivery system, Biol Pharm Bull. 31 (7) (2008) 1439–1443.
[21] M.R. Prausnitz, R. Langer, Transdermal drug delivery, Nat. Biotechnol. 26 (11) (2008) 1261–1268.
[22] W. Song, P. Quan, S. Li, C. Liu, S. Lv, Y. Zhao, et al., Probing the role of chemical enhancers in facilitating drug release from patches: mechanistic insights based on FT-IR spectroscopy, molecular modeling and thermal analysis, J Control Release. 227 (2016) 13–22.
[23] M.E. Lane, Skin penetration enhancers, Int. J. Pharm. 447 (1) (2013) 12–21.
[24] D. Ameen, B. Michniak-Kohn, Transdermal delivery of dimethyl fumarate for Alzheimer's disease: effect of penetration enhancers, Int. J. Pharm. 529 (1) (2017) 465–473.
[25] I. Diez, C. Peraire, R. Obach, J. Domenech, Influence of d-limonene on the transdermal penetration of felodipine, Eur J Drug Metab Pharmacokinet. 23 (1) (1998) 7–12.
[26] A.C. Williams, B.W. Barry, Penetration enhancers, Adv. Drug Deliv. Rev. 64 (Supplement) (2012) 128–137.
[27] P.J. Lee, N. Ahmad, R. Langer, S. Mitragotri, Shastri V. Prasad, Evaluation of chemical enhancers in the transdermal delivery of lidocaine, Int. J. Pharm. 308 (1) (2006) 33–39.
[28] H.S. Gwak, I.K. Chun, Effect of vehicles and penetration enhancers on the in vitro percutaneous absorption of tenoxicam through hairless mouse skin, Int. J. Pharm. 236 (1) (2002) 57–64.
[29] G.G. Agyralides, P.P. Dallas, D.M. Rekkas, Development and in vitro evaluation of furosemide transdermal formulations using experimental design techniques, Int. J. Pharm. 281 (1) (2004) 35–43.
[30] I. Kakubari, H. Sasaki, T. Takayasu, H. Yamauchi, S. Takayama, K. Takayama, Effects of ethylcellulose and 2-octyldodecanol additives on skin permeation and irritation with ethylene-vinyl acetate copolymer matrix patches containing formoterol fumarate, Biol. Pharm. Bull. 29 (8) (2006) 1717–1722.
[31] R. Ravula, A.K. Herwadkar, M.J. Abla, J. Little, A.K. Banga, Formulation optimization of a drug in adhesive transdermal analgesic patch, Drug Dev. Ind. Pharm. 42

(6) (2016) 862–870.
[32] M. Michaelis, C.S. Leopold, Mixture design approach for early stage formulation development of a transdermal delivery system, Drug Dev. Ind. Pharm. 41 (9) (2015) 1532–1540.
[33] V. Sachdeva, Y. Bai, A. Kydonieus, A.K. Banga, Formulation and optimization of desogestrel transdermal contraceptive patch using crystallization studies, Int. J. Pharm. 441 (1–2) (2013) 9–18.
[34] P. Jain, A.K. Banga, Induction and inhibition of crystallization in drug-in-adhesive-type transdermal patches, Pharm. Res. 30 (2) (2013) 562–571.
[35] P. Karande, S. Mitragotri, Enhancement of transdermal drug delivery via synergistic action of chemicals. Biochimica et Biophysica Acta (BBA) -, Biomembranes 1788 (11) (2009) 2362–2373.
[36] N.S. Thomas, R. Panchagnula, Combination strategies to enhance transdermal permeation of zidovudine (AZT), Pharmazie 58 (12) (2003) 895–898.
[37] C. Yao, A. Raoufinia, M. Gold, J.S. Nye, S. Ramael, M. Padmanabhan, et al., Steady-state pharmacokinetics of galantamine are not affected by addition of memantine in healthy subjects, J. Clin. Pharmacol. 45 (5) (2005) 519–528.
[38] C. Zhao, P. Quan, C. Liu, Q. Li, L. Fang, Effect of isopropyl myristate on the viscoelasticity and drug release of a drug-in-adhesive transdermal patch containing blonanserin, Acta Pharmaceutica Sinica B. 6 (6) (2016) 623–628.
[39] X. Huang, C.S. Brazel, On the importance and mechanisms of burst release in matrix-controlled drug delivery systems, J. Control. Release 73 (2) (2001) 121–136.
[40] M.S. Mufamadi, Y.E. Choonara, P. Kumar, G. Modi, D. Naidoo, S. van Vuuren, et al., Ligand-functionalized nanoliposomes for targeted delivery of galantamine, Int. J. Pharm. 448 (1) (2013) 267–281.
[41] K.Y. Ho, K. Dodou, Rheological studies on pressure-sensitive silicone adhesives and drug-in-adhesive layers as a means to characterise adhesive performance, Int J Pharm. 333 (1–2) (2007) 24–33.
[42] S. Venkatraman, R. Gale, Skin adhesives and skin adhesion. 1. Transdermal drug delivery systems, Biomaterials 19 (13) (1998) 1119–1136.
[43] N. Li, P. Quan, X. Wan, C. Liu, X. Liu, L. Fang, Mechanistic insights of the enhancement effect of sorbitan monooleate on olanzapine transdermal patch both in release and percutaneous absorption processes, Eur. J. Pharm. Sci. 107 (2017) 138–147.
[44] C. Liu, P. Quan, S. Li, Y. Zhao, L. Fang, A systemic evaluation of drug in acrylic pressure sensitive adhesive patch in vitro and in vivo: The roles of intermolecular interaction and adhesive mobility variation in drug controlled release, J. Control. Release 252 (2017) 83–94.